

HIGGS RADIATION OFF QUARKS IN SUPERSYMMETRIC THEORIES AT e^+e^- COLLIDERS

S. DITTMAIER¹, M. KRÄMER^{2*}, Y. LIAO^{3,4},
M. SPIRA^{5†} AND P.M. ZERWAS⁴

¹ Theoretische Physik, Universität Bielefeld, D-33615 Bielefeld, Germany

² Dept. of Physics and Astronomy, Univ. of Edinburgh, Edinburgh EH9 3JZ, Scotland

³ Department of Modern Applied Physics, Tsinghua University, Beijing 100084, PR China

⁴ DESY, Deutsches Elektronen-Synchrotron, D-22603 Hamburg, Germany

⁵ II. Institut für Theoretische Physik*, Universität Hamburg, D-22761 Hamburg, Germany

Abstract

Yukawa couplings between Higgs bosons and quarks in supersymmetric theories can be measured in the processes $e^+e^- \rightarrow Q\bar{Q} + \text{Higgs}$. We have determined the cross sections of these processes in the minimal supersymmetric model including the complete set of next-to-leading order QCD corrections for all channels.

*Supported by the EU FF Programme under contract FMRX-CT98-0194 (DG 12 - MIHT).

†Heisenberg-Fellow

1. In the Standard Model (SM) and its supersymmetric extensions, the masses of electroweak gauge bosons, leptons, and quarks are generated by interactions with Higgs fields [1]. The Yukawa couplings between Higgs particles and fermions therefore grow with the masses M_f of the fermions. The couplings obey a universal scaling law $g_{ffH} = M_f/v$ in the SM, with $v \approx 246$ GeV being the ground-state value of the Higgs field. In supersymmetric models, which involve at least two Higgs doublets, the size of the Yukawa couplings is also set by the fermion masses, yet the relationship is more complex owing to the mixing among the Higgs fields. The Yukawa couplings [2] of the two CP-even light/heavy Higgs bosons h/H and of the CP-odd Higgs boson A in the minimal supersymmetric extension of the Standard Model (MSSM) [3,4], expressed in units of the SM couplings, are collected in Table 1¹. The parameter $\tan\beta = v_2/v_1$ is the ratio of the vacuum expectation values

ϕ	$u\bar{u}\phi$	$d\bar{d}\phi$	$ZZ\phi$	$ZA\phi$
h	$\cos\alpha/\sin\beta$	$-\sin\alpha/\cos\beta$	$\sin(\beta-\alpha)$	$\cos(\beta-\alpha)$
H	$\sin\alpha/\sin\beta$	$\cos\alpha/\cos\beta$	$\cos(\beta-\alpha)$	$-\sin(\beta-\alpha)$
A	$1/\tan\beta$	$\tan\beta$	—	—

Table 1: *Higgs Yukawa couplings in the MSSM in units of the SM couplings M_f/v , and gauge couplings in units of the ZZH coupling M_Z/v in the SM.*

of the two Higgs fields generating the masses of up- and down-type particles, and α is the mixing angle in the CP-even sector. In the decoupling limit, in which the light Higgs mass reaches the maximum value for a given parameter $\tan\beta$, the h Yukawa couplings approach the SM values. In general, they are suppressed for up-type fermions and enhanced for down-type fermions; the enhancement increases with $\tan\beta$ and can therefore be very strong.

Higgs radiation off top or off bottom quarks in e^+e^- collisions,

$$e^+e^- \rightarrow Q\bar{Q}h/H/A \quad [Q = t, b], \quad (1)$$

lends itself as a suitable process for measuring the Yukawa couplings in supersymmetric theories [6], particularly for the light Higgs boson h and for moderately heavy Higgs bosons H and A . In this letter we present the cross sections for these processes including the next-to-leading order (NLO) QCD corrections. This problem has been solved before in the SM, where the QCD corrections significantly increase the cross section at moderate collider energies [7,8]. Moreover, it has been shown in detailed simulations that the SM top-quark Yukawa coupling can be measured with an accuracy close to 5% [9] (see also Ref. [10]) in high-luminosity operations of e^+e^- linear colliders. For the MSSM, first steps towards an NLO analysis have been made in Ref. [11], adopting either a global K factor from

¹For large $\tan\beta$, SUSY loop corrections to the $b\bar{b}$ -Higgs vertices become very important [5]. In the present QCD analysis, these corrections can be absorbed into effective Higgs Yukawa couplings, since emission and reabsorption of virtual heavy SUSY particles is confined to small space-time regions compared with QCD subprocesses involving massless gluons.

SM analyses or applying the QCD corrections to the cross sections for double resonance production in the narrow-width approximation. In the present analysis we have calculated the complete set of $\mathcal{O}(\alpha_s)$ QCD corrections to all subchannels in (1) systematically. The large number of interfering subchannels in supersymmetric theories renders this program more complex than the corresponding calculation in the SM, cf. Fig. 1, in particular since the relative weight of the subchannels varies over the supersymmetric parameter space and over the phase space for different mass ratios.

2. Examining the set of subchannels in Fig. 1, the QCD corrections can be categorized into five classes. Virtual corrections of the internal quark lines, of the γ/Z -quark vertices, of the scalar/pseudoscalar-Higgs-quark vertices, and box diagrams interfere with the Born amplitude. Gluon radiation off internal and external quark lines adds incoherently to the cross sections. In order to disentangle the different subchannels with couplings varying over the supersymmetric parameter space, the cross section for scalar Higgs radiation must be split into nine parts: Higgs radiation off the quarks (σ_1, σ_2), Higgs-strahlung off the Z -boson line (σ_3, σ_4), the related interference terms (σ_5, σ_6), real/virtual A decay (σ_7), and the interference with the first two Higgs-radiation and Higgs-strahlung channels (σ_8, σ_9):

$$\begin{aligned}
\sigma[e^+e^- \rightarrow Q\bar{Q}H_i(g)] = & \\
N_C \frac{\sigma_0}{4\pi} \left\{ \frac{(\hat{v}_e^2 + \hat{a}_e^2)}{(1 - M_Z^2/s)^2} \frac{g_{QQH_i}^2}{4\pi} (\hat{v}_Q^2 \sigma_1 + \hat{a}_Q^2 \sigma_2) + \left(Q_e^2 Q_Q^2 + \frac{2Q_e Q_Q \hat{v}_e \hat{v}_Q}{1 - M_Z^2/s} \right) \frac{g_{QQH_i}^2}{4\pi} \sigma_1 \right. & \\
+ \frac{(\hat{v}_e^2 + \hat{a}_e^2)}{(1 - M_Z^2/s)^2} \frac{g_{ZZH_i}^2}{4\pi} (\hat{v}_Q^2 \sigma_3 + \hat{a}_Q^2 \sigma_4) & \\
+ \frac{(\hat{v}_e^2 + \hat{a}_e^2)}{(1 - M_Z^2/s)^2} \frac{g_{QQH_i} g_{ZZH_i}}{4\pi} (\hat{v}_Q^2 \sigma_5 + \hat{a}_Q^2 \sigma_6) + \frac{Q_e Q_Q \hat{v}_e \hat{v}_Q}{1 - M_Z^2/s} \frac{g_{QQH_i} g_{ZZH_i}}{4\pi} \sigma_5 & \\
+ \frac{(\hat{v}_e^2 + \hat{a}_e^2)}{(1 - M_Z^2/s)^2} \frac{1}{4s_{2W}^2} \frac{g_{QQA}^2 g_{ZAH_i}^2}{4\pi} \sigma_7 & \\
+ \left. \frac{(\hat{v}_e^2 + \hat{a}_e^2)}{(1 - M_Z^2/s)^2} \frac{\hat{a}_Q}{2s_{2W}} \left(\frac{g_{QQA} g_{ZAH_i} g_{ZZH_i}}{4\pi} \sigma_8 + \frac{g_{QQA} g_{ZAH_i} g_{QQH_i}}{4\pi} \sigma_9 \right) \right\}, & \quad (2)
\end{aligned}$$

where $H_i = h, H$. Correspondingly, the cross section for pseudoscalar Higgs radiation may be written as

$$\begin{aligned}
\sigma[e^+e^- \rightarrow Q\bar{Q}A(g)] = & \\
N_C \frac{\sigma_0}{4\pi} \left\{ \frac{(\hat{v}_e^2 + \hat{a}_e^2)}{(1 - M_Z^2/s)^2} \frac{g_{QQA}^2}{4\pi} (\hat{v}_Q^2 \sigma'_1 + \hat{a}_Q^2 \sigma'_2) + \left(Q_e^2 Q_Q^2 + \frac{2Q_e Q_Q \hat{v}_e \hat{v}_Q}{1 - M_Z^2/s} \right) \frac{g_{QQA}^2}{4\pi} \sigma'_1 \right. & \\
+ \frac{(\hat{v}_e^2 + \hat{a}_e^2)/(4s_{2W}^2)}{(1 - M_Z^2/s)^2} \left(\frac{g_{QQh}^2 g_{ZAh}^2}{4\pi} \sigma'_3 + \frac{g_{QQH}^2 g_{ZAH}^2}{4\pi} \sigma'_4 + \frac{g_{QQh} g_{ZAh} g_{QQH} g_{ZAH}}{4\pi} \sigma'_5 \right) & \\
+ \left. \frac{(\hat{v}_e^2 + \hat{a}_e^2)}{(1 - M_Z^2/s)^2} \frac{\hat{a}_Q}{2s_{2W}} \left(\frac{g_{QQA} g_{QQh} g_{ZAh}}{4\pi} \sigma'_6 + \frac{g_{QQA} g_{QQH} g_{ZAH}}{4\pi} \sigma'_7 \right) \right\}, & \quad (3)
\end{aligned}$$

split into A radiation off the quarks (σ'_1, σ'_2), virtual Higgs decays (σ'_3, σ'_4) and their interference term (σ'_5), as well as their interference terms with the radiation diagrams (σ'_6, σ'_7). The Yukawa and gauge couplings are set off explicitly in (2) and (3), with the normalized couplings g_{QQH_i} etc. given in Table 1². The electric charges are defined as $Q_e = -1$, $Q_t = +2/3$ and $Q_b = -1/3$, and $\hat{v}_{e,Q}$ and $\hat{a}_{e,Q}$ are the vector and axial-vector charges of the electron and the quark Q , normalized as $\hat{v} = (I_{3L} - 2Qs_W^2)/s_{2W}$ and $\hat{a} = I_{3L}/s_{2W}$, with $I_{3L} = \pm 1/2$ being the weak isospin of the left-handed fermions [as usual, $s_W^2 = 1 - c_W^2 = \sin^2 \theta_W = 0.23$ and $s_{2W} = \sin 2\theta_W$]; $\sigma_0 = 4\pi\alpha^2/3s$ denotes the standard electromagnetic μ -pair cross section, and $N_C = 3$ is the color factor of the quarks. The value of the electromagnetic coupling is taken to be $\alpha = 1/128$. The mass of the Z boson is set to $M_Z = 91.187$ GeV, and the pole masses of the top and bottom quarks are set to $M_t = 174$ GeV [12] and³ $M_b = 4.62$ GeV [13], respectively. The masses of the MSSM Higgs bosons and their couplings are related to $\tan \beta$ and the pseudoscalar Higgs boson mass M_A . In the relation we use, higher-order corrections up to two loops in the effective-potential approach are included [14]. The SUSY parameters are chosen as $\mu = A_t = A_b = 0$ and $M_{\tilde{Q}} = 1$ TeV; this simple choice is sufficient to illustrate the main results.

The production of $b\bar{b}h/H/A$ final states in (2) and (3) can be mediated by resonance channels $e^+e^- \rightarrow Ah/H$ and Zh/H . We describe the resonance structures as Breit-Wigner forms by substituting $M^2 \rightarrow M^2 - iM\Gamma$ in all boson propagators. The decay widths of the Higgs bosons are calculated including higher-order corrections, as described in Refs. [15,16], while the Z width is set to $\Gamma_Z = 2.49$ GeV. For $t\bar{t}h/H/A$ production the widths can be neglected, since the Higgs masses are taken below the $t\bar{t}$ threshold.

The coefficients σ_i, σ'_i in the cross sections (2) and (3) can be decomposed into Born contributions $\sigma_i^0, \sigma_i'^0$ and QCD corrections δ_i, δ'_i :

$$\sigma_i = \sigma_i^0 \left(1 + \frac{\alpha_s}{\pi} \delta_i \right), \quad \sigma'_i = \sigma_i'^0 \left(1 + \frac{\alpha_s}{\pi} \delta'_i \right). \quad (4)$$

The renormalization scale of the QCD coupling α_s , which is evaluated in NLO with five active flavors normalized to $\alpha_s(M_Z^2) = 0.119$ [12], is chosen at $\mu_R^2 = s$, where $s = E_{\text{CM}}^2$ is the center-of-mass (CM) energy squared. By definition, the Yukawa couplings in the Born contributions are evaluated at the scale set by the Higgs momentum flow to leading logarithmic order.

The QCD radiative corrections have been calculated in the standard way. The Feynman diagrams and the amplitudes for the virtual corrections have been generated with *FeynArts* [17]. They have been evaluated by applying the standard techniques for one-loop calculations, as described in Refs. [18,19]. Ultraviolet divergences are consistently regularized in $D = 4 - 2\epsilon$ dimensions, with γ_5 treated naively since no anomalies are involved. The renormalization of the $Q\bar{Q}\phi$ vertices is connected to the renormalization of the quark masses, which, in the case of the top quark, is defined on shell (see e.g.

²The couplings $g_{QQ\phi}$ ($g_{ZZ\phi}, g_{ZA\phi}$) include the normalization coefficients M_Q/v (M_Z/v), respectively.

³This value for the perturbative pole mass of the bottom quark corresponds in NLO to an $\overline{\text{MS}}$ mass $\overline{m}_b(\overline{m}_b) = 4.28$ GeV.

Refs. [19,20] for details). Large logarithms are mapped into the running mass $\overline{m}_b(Q_{\text{Higgs}}^2)$ for the Yukawa couplings of the b quark, with Q_{Higgs}^2 denoting the squared momentum flow through the corresponding Higgs-boson line. The algebraic part of the virtual corrections has also been checked by using *FeynCalc* [21]. The infrared divergences encountered in the virtual corrections and in the cross section for real gluon emission, are treated in two different ways. Both calculations follow subtraction procedures, one using dimensional regularization and one introducing an infinitesimal gluon mass [22]. The results obtained by the two different procedures are in mutual numerical agreement after adding the contributions from virtual gluon exchange and real gluon emission. A second, completely independent calculation of the QCD corrections to the total cross section was based on the evaluation of all relevant cut diagrams of the photon and Z -boson self-energies in two-loop order, generalizing the method applied to $t\bar{t}(g)$ intermediate states in Ref. [23]. The results of the two approaches are in numerical agreement. The final expressions for the integrated cross sections σ_i^0 , $\sigma_i^{\prime 0}$ and for the QCD corrections δ_i , δ_i' are, however, too lengthy to be recorded in this letter⁴.

3. The general characteristics of the reactions (1) will be discussed for two examples in detail, $\tan\beta = 3$ and 30. The numerical analysis has been performed for the case of no mixing in the stop and sbottom sectors of the MSSM. Since the top Yukawa couplings are suppressed for large values of $\tan\beta$, sizeable cross sections for $t\bar{t}\phi$ production are expected only for small and moderate values of $\tan\beta$ and in the decoupling regime at large values of $\tan\beta$, where the h couplings approach the SM values. The opposite is realized for $b\bar{b}\phi$ production outside the resonance regions due to the strong enhancement of the b Yukawa couplings for large values of $\tan\beta$.

a.) The QCD corrections to the top final states $t\bar{t}\phi$ can be interpreted easily in two kinematical areas. Whenever the invariant mass of the $t\bar{t}$ pair is close to threshold, the gluonic Sommerfeld rescattering-correction is positive and becomes large. In the threshold region the K factor approaches the asymptotic form [7]

$$K_{\text{thr}}^{t\bar{t}\phi} \rightarrow 1 + \frac{32\alpha_s}{9\beta_t} \quad (5)$$

with the maximal quark velocity $\beta_t = \sqrt{(\sqrt{s} - M_\phi)^2 - 4M_t^2}/2M_t$ in the $(t\bar{t})$ rest frame.

For high energies, on the other hand, the QCD corrections are of order α_s/π . In the energy region $s \gg 4M_t^2 \gg M_H^2$ but $\log s/M_t^2 \not\gg \mathcal{O}(1)$, which is relevant for the present analysis, the QCD corrections can qualitatively be traced back to vertex corrections and infrared gluon radiation. Since scalar Higgs bosons are radiated off top quarks preferentially with small energy [$x = E_\phi/E_t \rightarrow 0$], as is evident from the leading (universal) part of the fragmentation function

$$f(t \rightarrow t h/H; x) = \frac{g_{tth/H}^2}{16\pi^2} \left[4 \frac{1-x}{x} + x \log \frac{s}{M_t^2} \right], \quad (6)$$

⁴NLO Fortran programs calculating the integrated cross sections and differential distributions for all the processes, are available on the web [24].

the QCD correction of the scalar Yukawa vertex, regularized by soft gluon radiation, approaches the value [8]

$$\Delta_{h/H}^{V+IR} = \frac{4\alpha_s}{3\pi} \left[-1 + \frac{2-x}{x} \log(1-x) \right] \rightarrow -4 \frac{\alpha_s}{\pi} . \quad (7)$$

The scalar Yukawa vertex is therefore reduced by four units in α_s/π which are compensated only partly by one unit due to the increase of the $t\bar{t}$ production probability, leading in total [7,8] to

$$K_{\text{cont}}^{t\bar{t}\phi} \rightarrow 1 - 3 \frac{\alpha_s}{\pi} + \dots \quad \text{for } \phi = h, H . \quad (8)$$

The ellipsis accounts for hard Higgs and gluon radiation (of order $+\alpha_s/\pi$). Thus, the QCD corrections are expected negative for scalar Higgs particles in the high energy continuum.

By contrast, the corresponding fragmentation function for the pseudoscalar Higgs boson [25]

$$f(t \rightarrow tA; x) = \frac{g_{ttA}^2}{16\pi^2} x \log \frac{s}{M_t^2} \quad (9)$$

is hard so that the average of the vertex and IR gluon corrections over the Higgs spectrum amounts to

$$\Delta_A^{V+IR} \rightarrow \frac{4\alpha_s}{3\pi} \left\langle \left[1 + \frac{2-x}{x} \log(1-x) \right] \right\rangle \sim -\frac{3}{2} \frac{\alpha_s}{\pi} . \quad (10)$$

Adding to this correction the increase of the $t\bar{t}$ production probability of one unit, the K factor is very close to unity

$$K_{\text{cont}}^{t\bar{t}A} \rightarrow 1 - \frac{1}{2} \frac{\alpha_s}{\pi} + \dots \quad (11)$$

After hard gluon bremsstrahlung is taken into account (symbolized by the ellipsis), the overall QCD corrections for the pseudoscalar Higgs boson are therefore expected slightly positive. [For ultra-high energies, i.e. $\log s/M_t^2 \gg 1$, hard gluon bremsstrahlung becomes important. Similarly to the leading terms in the fragmentation functions eqs. (6) and (9), the QCD corrections for scalar and pseudoscalar Higgs bosons approach each other as a result of chiral symmetry restoration in *asymptotia*; this has been verified in a numerical calculation.]

Similar estimates can be applied to bottom final states which in general are dominated by resonance decays. After absorbing the large logarithms $\log(Q_\phi^2/M_b^2)$ into the Yukawa couplings, the non-leading effects are positive:

$$K_{\text{res}}^{b\bar{b}\phi} \approx 1 + \left\{ \frac{17}{3}, 1 \right\} \frac{\alpha_s}{\pi} \quad \text{for } \{\text{Higgs}, Z\} \rightarrow b\bar{b} . \quad (12)$$

Also close to the thresholds and in the high-energy limit the QCD corrections remain positive after mapping the large (negative) corrections into the running Yukawa couplings. Since different channels are activated at the same time, only a qualitative estimate can be given in the continuum regime,

$$K_{\text{cont}}^{b\bar{b}\phi} = 1 + c \frac{\alpha_s}{\pi} \quad \text{with } c = \mathcal{O}(1), \quad (13)$$

while details must be left to the numerical analysis.

b.) The results are exemplified in Fig. 2 for $\tan\beta = 3$ and 30 and for the collider energy $E_{\text{CM}} = 500$ GeV. If required by the size of the cross section, which should not fall below $\sim 10^{-2}$ fb in order to be accessible experimentally, we switched to $E_{\text{CM}} = 1$ TeV. The Born terms are shown by the dotted curves, while the final results for the cross sections, including QCD corrections, are given by the full curves.

For $E_{\text{CM}} = 500$ GeV the QCD corrections to Higgs-boson production in association with $t\bar{t}$ pairs increase the scalar Higgs-production cross sections significantly, as can be inferred from Fig. 2. Close to threshold the numerical results clearly exhibit the strong increase of the cross sections due to the Coulomb singularity (5). Moreover, for $\tan\beta = 30$ the cross sections are strongly suppressed except for the regions where the light (heavy) scalar Higgs mass is close to its upper (lower) bound. For $\tan\beta = 3$ the cross section amounts to about 1 fb, which leads to a significant number of events at the TESLA collider, being designed to reach integrated luminosities of about $\int \mathcal{L} \sim 1$ ab $^{-1}$ in three years of operation.

For CM energies of 1 TeV the QCD corrections to scalar Higgs production in association with $t\bar{t}$ pairs are of moderate size. They decrease the cross sections by about 3–5%. This is in accordance with the asymptotic form of the K factor [7]. For pseudoscalar Higgs production, the size of the QCD corrections is slightly positive at 1 TeV, in agreement with the qualitative discussion above.

The cross sections for Higgs-boson production associated with $b\bar{b}$ pairs are significantly larger due to the resonance contributions from on-shell Z and Higgs-boson decays into $b\bar{b}$ pairs. The QCD corrections increase these cross sections by about 5–25%. The drop in the $b\bar{b}A$ production cross section for $\tan\beta = 3$ at $M_A \sim 140$ GeV and 175 GeV can be attributed to the crossing of the thresholds for resonant $H \rightarrow WW$ and $H \rightarrow hh$ decays, respectively, in HA final states.

Without cuts, the intermediate resonance decays $Z, h, H, A \rightarrow b\bar{b}$ dominate all $b\bar{b}\phi$ production processes, whenever they are kinematically allowed, and it will be difficult to extract the bottom Yukawa couplings experimentally in regions where resonant Higgs decays to $b\bar{b}$ pairs are dominant. This is the case at large values of $\tan\beta$ for all neutral Higgs particles and at small values of $\tan\beta$ for Higgs masses below the WW threshold. In these cases the branching ratios, which determine the size of the $b\bar{b}\phi$ cross sections, will be nearly independent of the bottom Yukawa couplings. Resonance decays $R \rightarrow b\bar{b}$ pairs in the $b\bar{b}h/H/A$ final states can however be eliminated by cutting out the resonance energy of the final-state Higgs boson, $E_{\phi,\text{res}} = (s + M_\phi^2 - M_R^2)/2\sqrt{s}$. After subtracting these resonance parts, the non-resonant contributions are suppressed by about one to three orders of magnitude. The resonances have been removed from the cross sections in the examples of Fig. 3 by subtracting the two-particle cross sections in the Breit–Wigner bands $M_R \pm \Delta$ of the energy $E_{\phi,\text{res}}$ with the resolution $\Delta = 5$ GeV. This theoretical definition is used for the sake of simplicity; wider cuts may be required in experimental analyses. Peaks and dips in the cross sections are the result of overlapping Breit-Wigner bands. For the scalar Higgs particles they arise from overlapping Z and A boson bands; in pseudoscalar Higgs production the light and heavy scalar resonance bands overlap for

100 GeV $\lesssim M_A \lesssim$ 120 GeV for $\tan\beta = 30$. The dips occur whenever the two resonance bands touch each other, while the peaks between the dips occur when the resonance masses coincide exactly. As shown in Fig. 3, the QCD-corrected cross sections are still close to 1 fb or slightly below, except for heavy masses at small values of $\tan\beta$. Thus, ensembles of order 10^3 events can be collected at a high-luminosity collider.

4. Measurements of Yukawa couplings in supersymmetric Higgs radiation off heavy quarks at e^+e^- linear colliders are difficult. This is a result of the large number of subchannels contributing to the $Q\bar{Q}h/H/A$ final states in supersymmetric theories in general, and the contamination by two-Higgs final states in particular. Nevertheless, the continuum cross sections appear large enough to approach this experimental problem as shown in the present analysis. Even though experimental simulations are beyond the scope of this note, it may be concluded from earlier SM analyses that the method will work at least in part of the MSSM parameter space, thus providing us with the absolute size of the quark–Higgs Yukawa couplings in the minimal supersymmetric theory.

Acknowledgement

Y.L. thanks Prof. A. Wagner for the warm hospitality extended to him during his visit at DESY, based on the DESY–Tsinghua cooperation contract.

References

- [1] P.W. Higgs, Phys. Lett. **12** (1964) 132; F. Englert and R. Brout, Phys. Rev. Lett. **13** (1964) 321; G.S. Guralnik, C.R. Hagen and T.W. Kibble, Phys. Rev. Lett. **13** (1964) 585.
- [2] J.F. Gunion and H.E. Haber, Nucl. Phys. **B272** (1986) 1 and **B278** (1986) 449; J.F. Gunion, H.E. Haber, G.L. Kane and S. Dawson, *The Higgs Hunters Guide*, Addison-Wesley 1990.
- [3] P. Fayet and S. Ferrara, Phys. Rep. **32** (1977) 249; H.P. Nilles, Phys. Rep. **110** (1984) 1; H.E. Haber and G.L. Kane, Phys. Rep. **117** (1985) 75; R. Barbieri, Riv. Nuovo Cim. **11** (1988) 1.
- [4] M. Spira and P.M. Zerwas, Lectures, 36th Int. Universitätswochen, Schladming 1997, [hep-ph/9803257].
- [5] L. Hall, R. Rattazzi and U. Sarid, Phys. Rev. **D50** (1994) 7048; R. Hempfling, Phys. Rev. **D49** (1994) 6168; M. Carena, M. Olechowski, S. Pokorski and C.E.M. Wagner, Nucl. Phys. **B426** (1994) 269; D. Pierce, J. Bagger, K. Matchev, and R. Zhang, Nucl. Phys. **B491** (1997) 3; M. Carena, S. Mrenna and C.E.M. Wagner, Phys. Rev. **D60**

- (1999) 075010; M. Carena, D. Garcia, U. Nierste and C.E.M. Wagner, Fermilab-Pub-99/367-T [hep-ph/9912516].
- [6] A. Djouadi, J. Kalinowski and P.M. Zerwas, *Mod. Phys. Lett.* **A7** (1992) 1765 and *Z. Phys.* **C54** (1992) 255.
- [7] S. Dittmaier, M. Krämer, Y. Liao, M. Spira and P.M. Zerwas, *Phys. Lett.* **B441** (1998) 383.
- [8] S. Dawson and L. Reina, *Phys. Rev.* **D57** (1998) 5851 and **D59** (1999) 054012.
- [9] A. Juste and G. Merino, Proceedings, Sitges Conference, Barcelona AU Report [hep-ph/9910301]; H. Baer, S. Dawson and L. Reina, FSU-HEP-990630 [hep-ph/9906419].
- [10] S. Moretti, *Phys. Lett.* **B452** (1999) 338.
- [11] S. Dawson and L. Reina, *Phys. Rev.* **D60** (1999) 015003.
- [12] C. Caso et al., Particle Data Group, *Eur. Phys. J.* **C3** (1998) 1.
- [13] S. Narison, *Phys. Lett.* **B341** (1994) 73; M. Jamin and A. Pich, *Nucl. Phys.* **B507** (1997) 334; M. Beneke and A. Signer, CERN-TH-99-163 [hep-ph/9906475].
- [14] M. Carena, M. Quirós and C.E.M. Wagner, *Nucl. Phys.* **B461** (1996) 407; H.E. Haber, R. Hempfling and A.H. Hoang, *Z. Phys.* **C75** (1997) 539; S. Heinemeyer, W. Hollik and G. Weiglein, *Phys. Rev.* **D58** (1998) 091701.
- [15] A. Djouadi, J. Kalinowski and P.M. Zerwas, *Z. Phys.* **C70** (1996) 435.
- [16] A. Djouadi, *Int. J. Mod. Phys.* **A10** (1995) 1; M. Spira, *Fortschr. Phys.* **46** (1998) 203; A. Djouadi, J. Kalinowski and M. Spira, *Comput. Phys. Commun.* **108** (1998) 56.
- [17] J. Küblbeck, M. Böhm and A. Denner, *Comput. Phys. Commun.* **60** (1990) 165; H. Eck and J. Küblbeck, *Guide to FeynArts 1.0*, Univ. Würzburg, 1992.
- [18] G. 't Hooft and M. Veltman, *Nucl. Phys.* **B153** (1979) 365; G. Passarino and M. Veltman, *Nucl. Phys.* **B160** (1979) 151.
- [19] A. Denner, *Fortschr. Phys.* **41** (1993) 307.
- [20] E. Braaten and J.P. Leveille, *Phys. Rev.* **D22** (1980) 715; M. Drees and K. Hikasa, *Phys. Lett.* **B240** (1990) 455; (E) **B262** (1991) 497.
- [21] R. Mertig, M. Böhm and A. Denner, *Comput. Phys. Commun.* **64** (1991) 345; R. Mertig, *Guide to FeynCalc 1.0*, Univ. Würzburg, 1992.
- [22] S. Dittmaier, BI-TP 99/09 [hep-ph/9904440], to appear in *Nucl. Phys.* **B**.

- [23] A. Djouadi and P. Gambino, Phys. Rev. **D49** (1994) 3499; (E) **D53** (1996) 4111.
- [24] DESY LC Physics home page: <http://www.desy.de/HEP/desy-hep.html>.
- [25] W. Beenakker, R. Höpker, M. Spira and P.M. Zerwas, Nucl. Phys. **B492** (1997) 51.

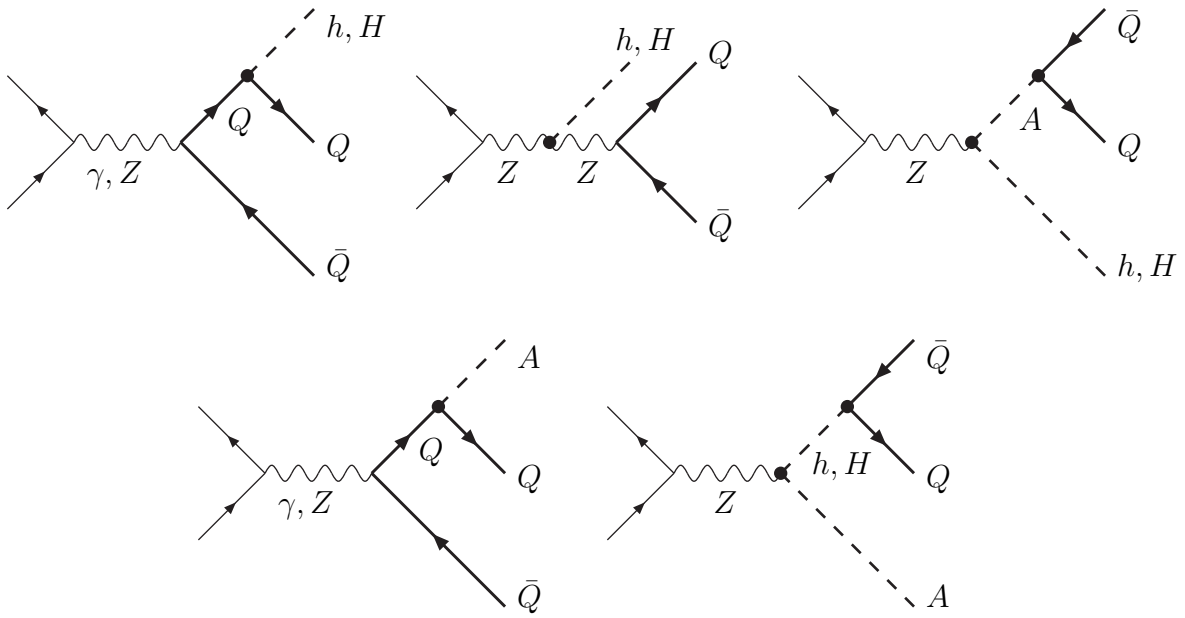


Figure 1: *Subchannels for the radiation of scalar and pseudoscalar MSSM Higgs bosons in e^+e^- collisions; $Q = t, b$.*

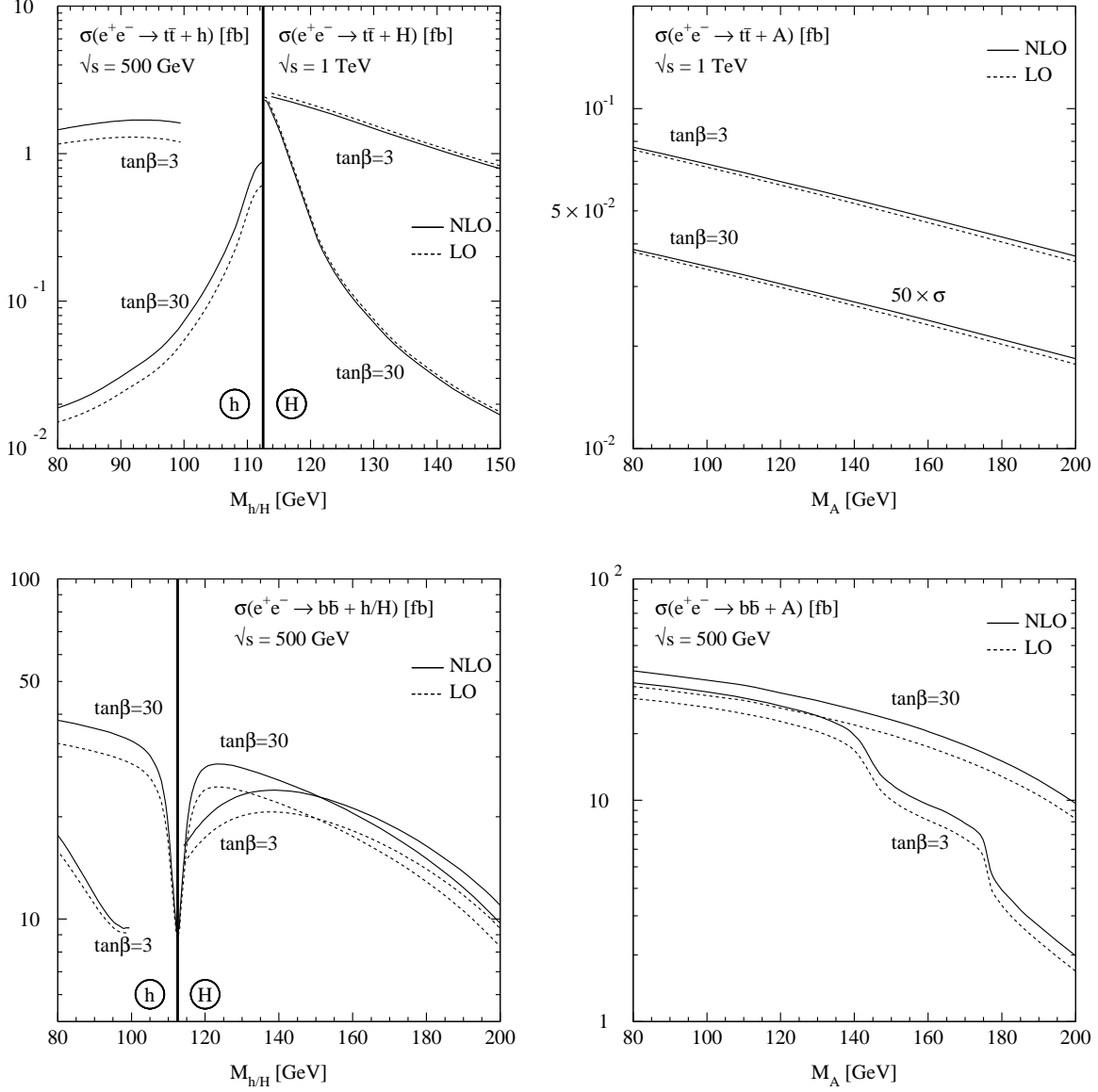


Figure 2: Production cross sections for the MSSM Higgs bosons h , H and A in association with heavy t, b quark pairs; Born approximation: dashed, QCD corrections included: full curves. The rapid drops in the $b\bar{b}A$ cross section at $\tan\beta = 3$ are due to the kinematical opening of the resonant $H \rightarrow WW, hh$ decays, which reduce the branching ratio of the resonant $H \rightarrow b\bar{b}$ decay.

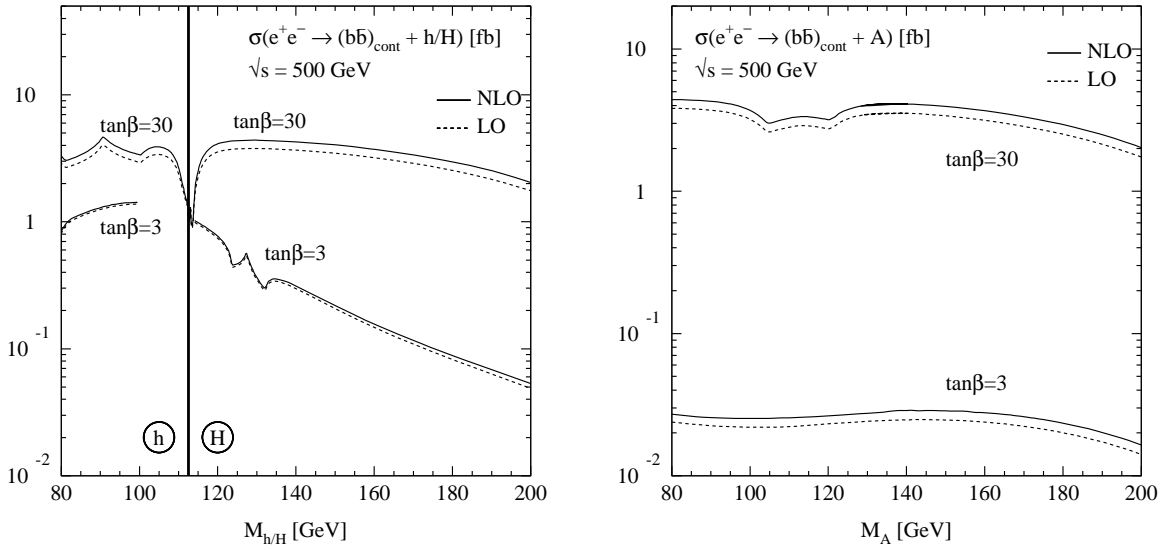


Figure 3: Continuum production of MSSM Higgs bosons h , H , A in association with a $b\bar{b}$ pair after subtraction of resonance decays to $b\bar{b}$ pairs in the Breit-Wigner bands $M_R \pm 5$ GeV.